

Supporting Information on

Exciton Coupling Dynamics in *Syn*- and *Anti*-type β - β Linked Zn(II) Porphyrin Linear Arrays

Taeyeon Kim,[†] Juwon Oh,[†] Hua-Wei Jiang,[‡] Takayuki Tanaka,[‡] Atsuhiko Osuka,^{*,‡} Dongho Kim,^{*,†}

[†]Spectroscopy Laboratory for Functional π - Electronic Systems and Department of Chemistry, Yonsei University, Seoul 120-749, Korea

[‡]Department of Chemistry, Graduate School of Science, Kyoto University, Sakyo-ku, Kyoto 606-8502, Japan

E-mail: dongho@yonsei.ac.kr (D. Kim); osuka@kuchem.kyoto-u.ac.jp (A. Osuka)

Table of Contents

1. Experimental details

2. Computational details

3. Supporting figures and table (Fig. S1–S10, Table S1)

4. References for supporting information

1. Experimental sections

Sample preparation.

Two types of β - β linked porphyrin arrays (**Sn** and **An**) were synthesized and the details in synthesis, and basic characterizations are provided with X-ray crystallographic analysis of dimer (**D**) and **A3**.¹

Steady-state measurements.

Steady-state absorption spectra were measured on a UV/Vis/NIR spectrometer (Varian, Cary5000) and fluorescence spectra were measured on a fluorescence spectrophotometer (Hitachi, F-2500). Fluorescence spectra are spectrally corrected by using correction factor of the fluorescence spectrophotometer. HPLC-grade solvents were purchased from Sigma-Aldrich and used without further purification. For the steady-state fluorescence excitation anisotropy measurement,

Glan laser and sheet polarizers were added into the excitation and monitoring paths, respectively. The calculation of anisotropy at specific monitoring wavelength (λ_{em}) as a function of excitation wavelength (λ_{ex}) was the given by

$$r(\lambda_{ex}) = \frac{I_{VV}(\lambda_{ex}) - GI_{VH}(\lambda_{ex})}{I_{VV}(\lambda_{ex}) + 2GI_{VH}(\lambda_{ex})} \quad (1)$$

where $I_{VV}(\lambda_{ex})$ (or $I_{VH}(\lambda_{ex})$) is the fluorescence intensity with the photoexcitation at λ_{ex} when the excitation light is vertically polarized and only the vertically (or horizontally) polarized portion of the fluorescence is detected, and the first and second subscripts represent excitation and detection polarizations, respectively. The factor of correction factor G is defined by $[I_{HV}(\lambda_{em}) / I_{HH}(\lambda_{em})]$, which is equal to the ratio of the sensitivity of the detection system for vertically and horizontally polarized light at given emission wavelength λ_{em} . Experimental G value was measured to be around 1.8 in our instrument. All steady-state measurements were carried out by using a quartz cuvette with a pathlength of 1 cm at ambient temperatures.

Picosecond time-resolved fluorescence measurements.

A time-correlated single-photon-counting (TCSPC) system was used for measurements of spontaneous fluorescence decay. As an excitation light source, we used a mode-locked Ti:sapphire laser (Spectra Physics, MaiTai BB) which provides ultrashort pulse (center wavelength of 800 nm with 80 fs at FWHM) with high repetition rate (80 MHz). This high repetition rate was reduced to 800 kHz by using homemade pulse-picker. The pulse-picked output was frequency doubled by a 1-mm-thick BBO crystal (type-I, $\theta = 29.2^\circ$, EKSMA). The fluorescence was collected by a microchannel plate photomultiplier (MCP-PMT, Hamamatsu, R3809U-51) with a thermoelectric cooler (Hamamatsu, C4878) connected to a TCSPC board (Becker & Hickel SPC-130). The overall instrumental response function was about 25 ps (FWHM). A vertically polarized pump pulse by a Glan-laser polarizer was irradiated to

samples, and a sheet polarizer set at an angle complementary to the magic angle (54.7°), was placed in the fluorescence collection path to obtain polarization-independent fluorescence decays.

Femtosecond transient absorption measurements.

A femtosecond time-resolved transient absorption (TA) spectrometer used for this study consisted of a femtosecond optical parametric amplifier (Quantronix, Palitra-FS) pumped by a Ti:sapphire regenerative amplifier system (Quantronix, Integra-C) operating at 1 kHz repetition rate and an accompanying optical detection system. The generated OPA pulses had a pulse width of ~100 fs and an average power of 1 mW in the range 550 to 690 nm, which were used as pump pulses. White light continuum (WLC) probe pulses were generated using a sapphire window (2 mm thick) by focusing of small portion of the fundamental 800 nm pulses, which were picked off by a quartz plate before entering into the OPA. The time delay between pump and probe beams was carefully controlled by making the pump beam travel along a variable optical delay (Newport, ILS250). Intensities of the spectrally dispersed WLC probe pulses were monitored by high speed spectrometer (Ultrafast Systems). To obtain the time-resolved transient absorption difference signal (ΔA) at a specific time, the pump pulses were chopped at 500 Hz and absorption spectra intensities were saved alternately with or without pump pulse. Typically, 6000 pulses were used to excite samples and to obtain the TA spectra at a particular delay time. The polarization angle between pump and probe beam was set at the magic angle (54.7°) using a Glan-laser polarizer with a half-wave retarder to prevent polarization-dependent signals. The cross-correlation FWHM in the pump-probe experiments was less than 200 fs, and chirp of WLC probe pulses was measured to be 800 fs in the 450-850 nm regions. To minimize chirp, all reflection optics were used in the probe beam path, and a quartz cell of 2 mm path length was employed. For time-resolved transient absorption anisotropy (TAA) measurement, both $\Delta A_{VV}(t)$ and $\Delta A_{VH}(t)$ signals were collected simultaneously by combination of polarizing beam-splitter cube and dual lock-in amplifiers as following equation;

$$r(t) = \frac{\Delta A_{VV}(t) - G\Delta A_{VH}(t)}{\Delta A_{VV}(t) + 2G\Delta A_{VH}(t)} \quad (3)$$

Where $\Delta A_{VV}(t)$ and $\Delta A_{VH}(t)$ represent TA signals with the polarization of the pump and probe pulses being mutually parallel and perpendicular, respectively. The pump pulsed was set to vertical polarization and that of probe pulse was set to 45° with respect to the pump pulse by using Glan-laser polarizers and half-wave plates. After the probe pulse passes through the samples cell, it was split by polarizing beam-splitter cube and then detected by two separate photodiodes. Two gated-integrators and two lock-in amplifiers record the signals simultaneously within a single scan. The correction factor G was obtained by taking into account the anisotropy of reference sample (ZnDPP monomer) falling into zero by rotational diffusion process. After completing each set of fluorescence and TA experiments, the absorption spectra of all compounds were carefully checked to rule out the presence of artifacts

or spurious signals arising from, for example, degradation or photo-oxidation of the samples in question.

2. Quantum mechanical calculations

Quantum mechanical calculations were carried out with Gaussian 09 program suite.² Geometry optimization in ground state (S_0) was performed by density functional theory (DFT) and time-dependent DFT (TD-DFT), respectively, method with CAM-B3LYP,³ employing a basis set consisting of 6-31G(d) for all atoms.⁴ To reduce the computational cost, two substituents in each porphyrin unit (3,5-di-tert-butylphenyl) are omitted.

3. Supporting figures

Optimized molecular structure

Optimized molecular structures of **Sn** and **An** were assumed from their crystal structures of **D** and **S3** as below. Other local minima structures are not discussed here for simplicity and it is appropriate to neglect other possible structures (such as **Sn** having dihedral angle similar to **An** and vice versa) because the exciton coupling strongly depends on the linkage position from our analysis through the paper, i.e. the relative orientation of porphyrin units to the long molecular axis is crucial and differs largely, zigzag in **Sn** and parallel in **An**.

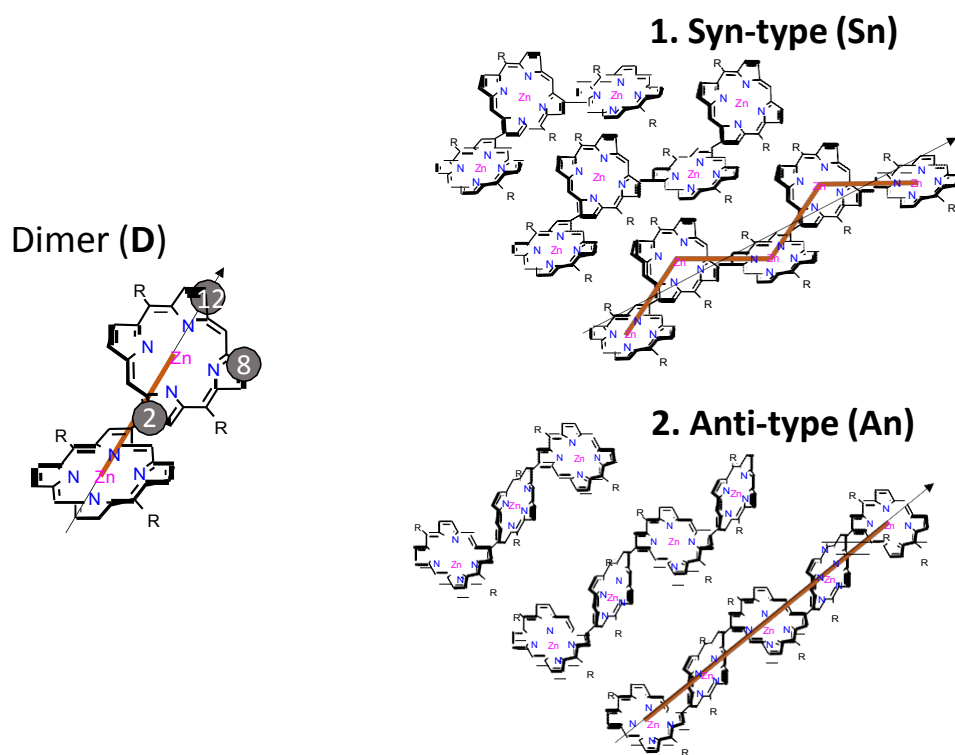


Fig. S1 Optimized structures of **D**, **Sn** and **An**. Arrows indicate the long molecular axes. Lines connect adjacent porphyrin units by center-to-center.

Gaussian fitted Q band absorption spectra

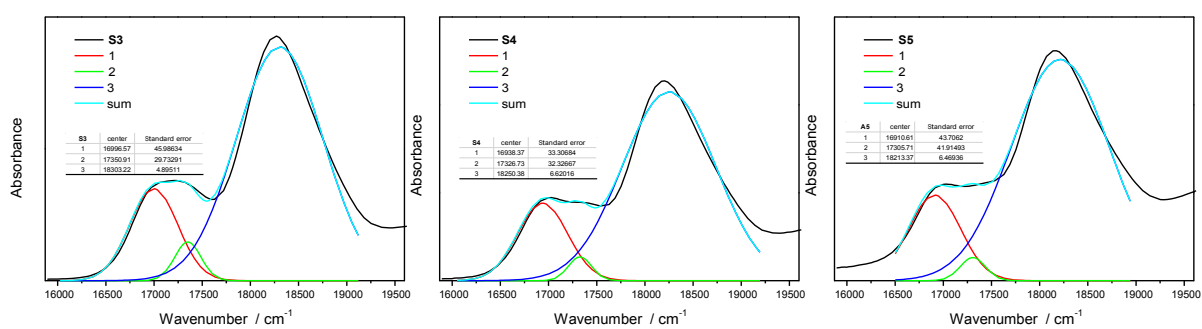


Fig. S2 Gaussian fitting for **S_n** in the Q band region are shown.

Detailed spectral data

	ϵ ($10^5 \text{ M}^{-1}\text{cm}^{-1}$)	Monomer-like peak	$Q_e(0,0)$
D	2.94 at 411 nm	411 nm	585 nm
S3	4.25 at 411 nm	411 nm	588 nm

S4	4.96 at 412 nm	412 nm	590 nm
S5	5.72 at 412 nm	412 nm	591 nm
A3	4.57 at 411 nm	411 nm	595 nm
A4	5.12 at 411 nm	411 nm	599 nm
A5	6.66 at 411 nm	411 nm	601 nm

Table. S1 Gaussian fitting for **Sn** in the Q band region are shown.

Gaussian fitted Q band absorption spectra

Fluorescence excitation spectra

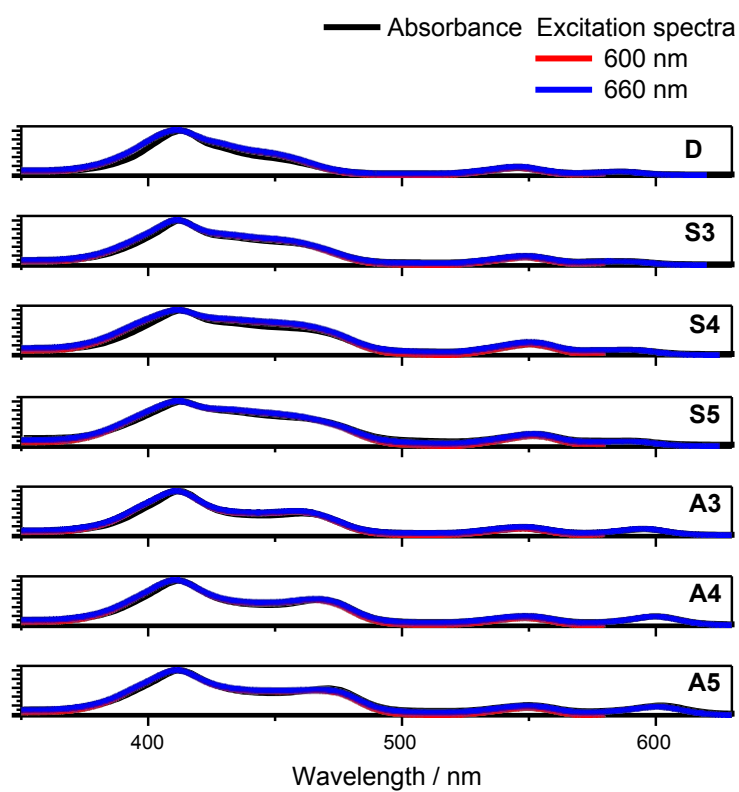


Fig. S3 Fluorescence excitation spectra of β - β linked porphyrin arrays are shown.

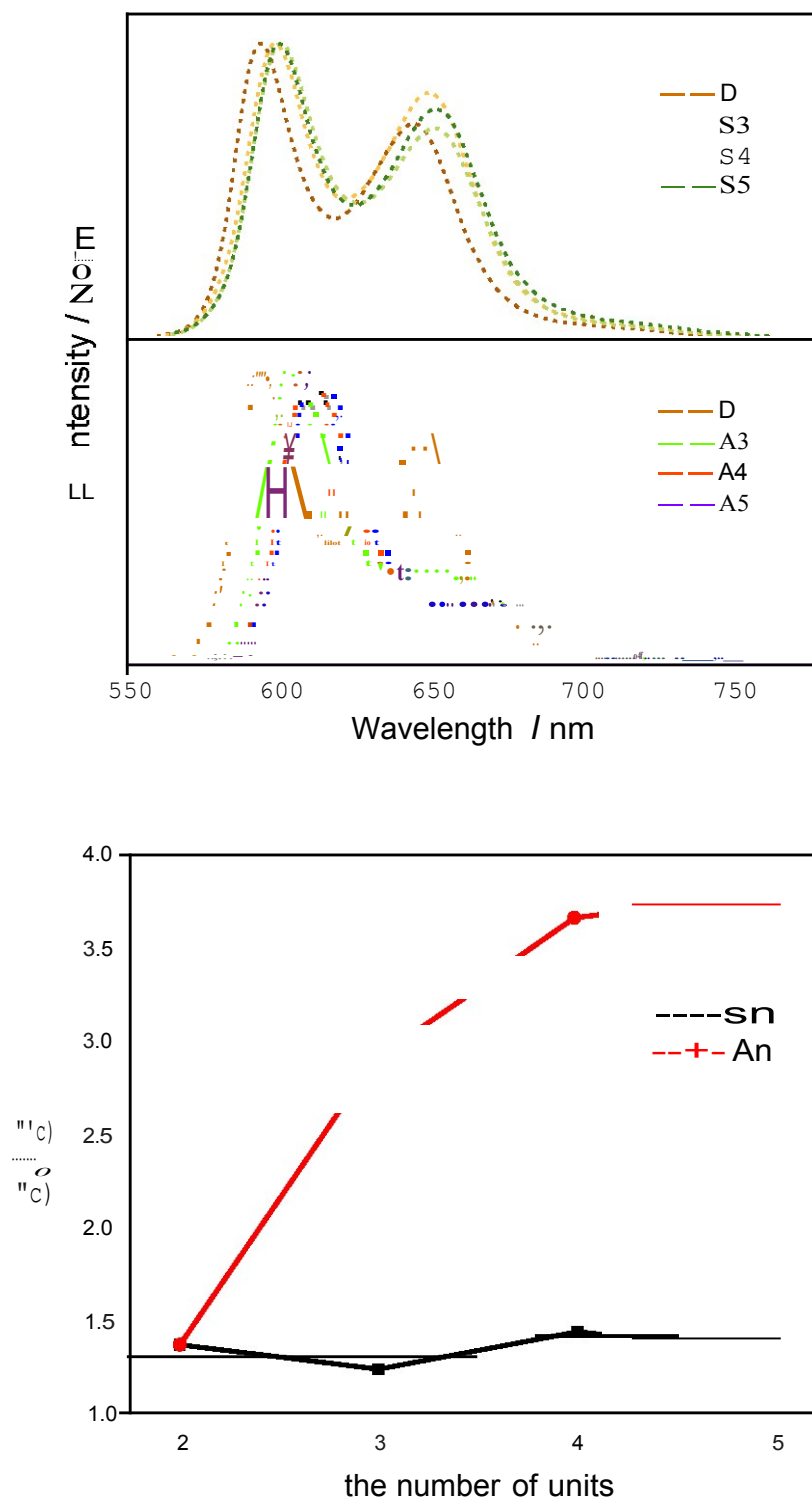


Fig. S4 Fluorescence spectra of Sn and An with comparing to dimer (top), vibronic peak ratios ($I_{0,0}/I_{0,1}$) in fluorescence spectra of Sn and An (bottom) are shown. Their peak intensities were obtained by assuming that each vibronic band is following Gaussian function.

Fluorescence spectra and vibronic peak ratios
 Fluorescence lifetime measurement by TCSPC

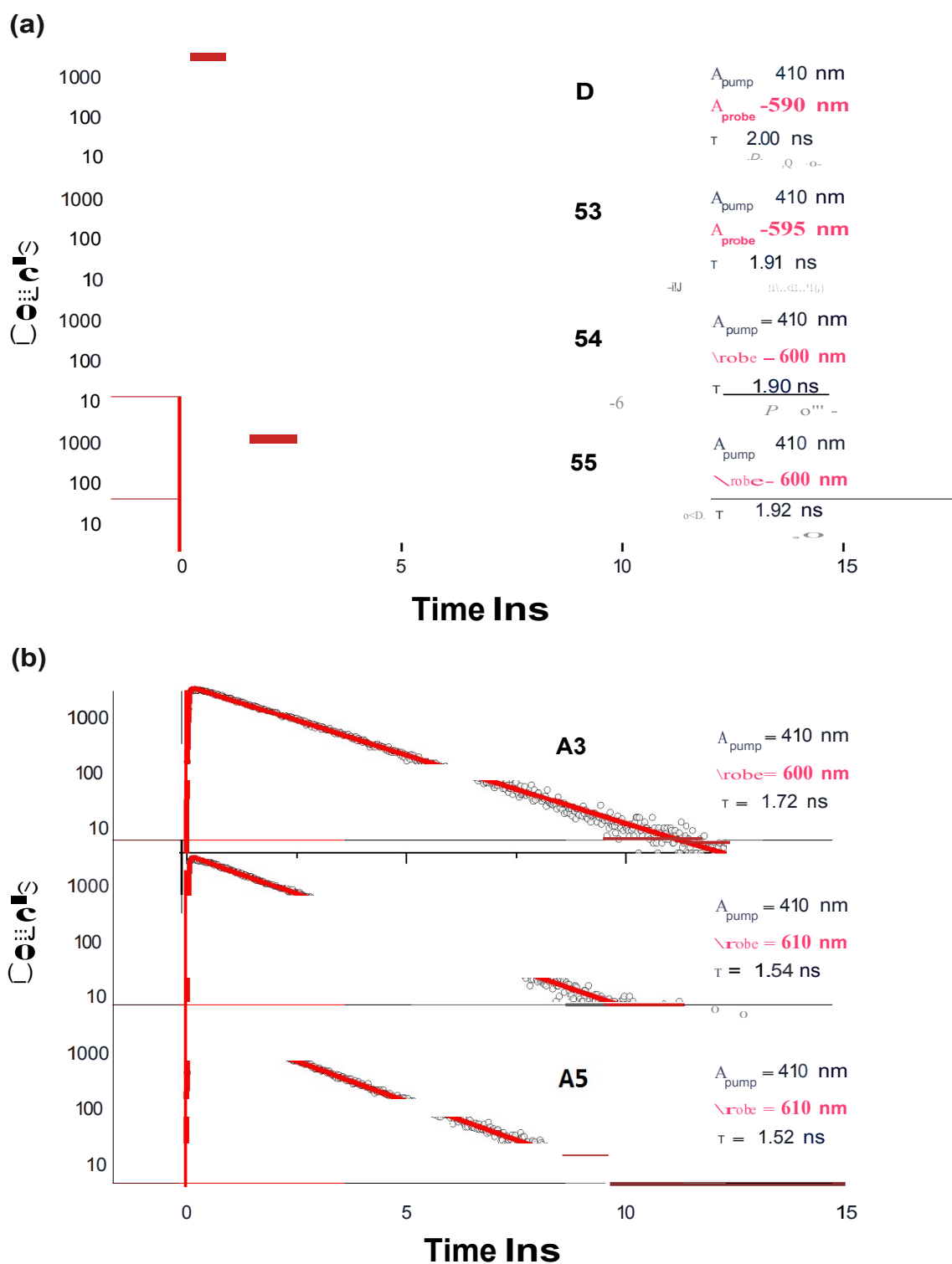


Fig. S5 Fluorescence lifetimes of **D**, **Sn**, and **An** were obtained from TCSPC measurement in dichloromethane.

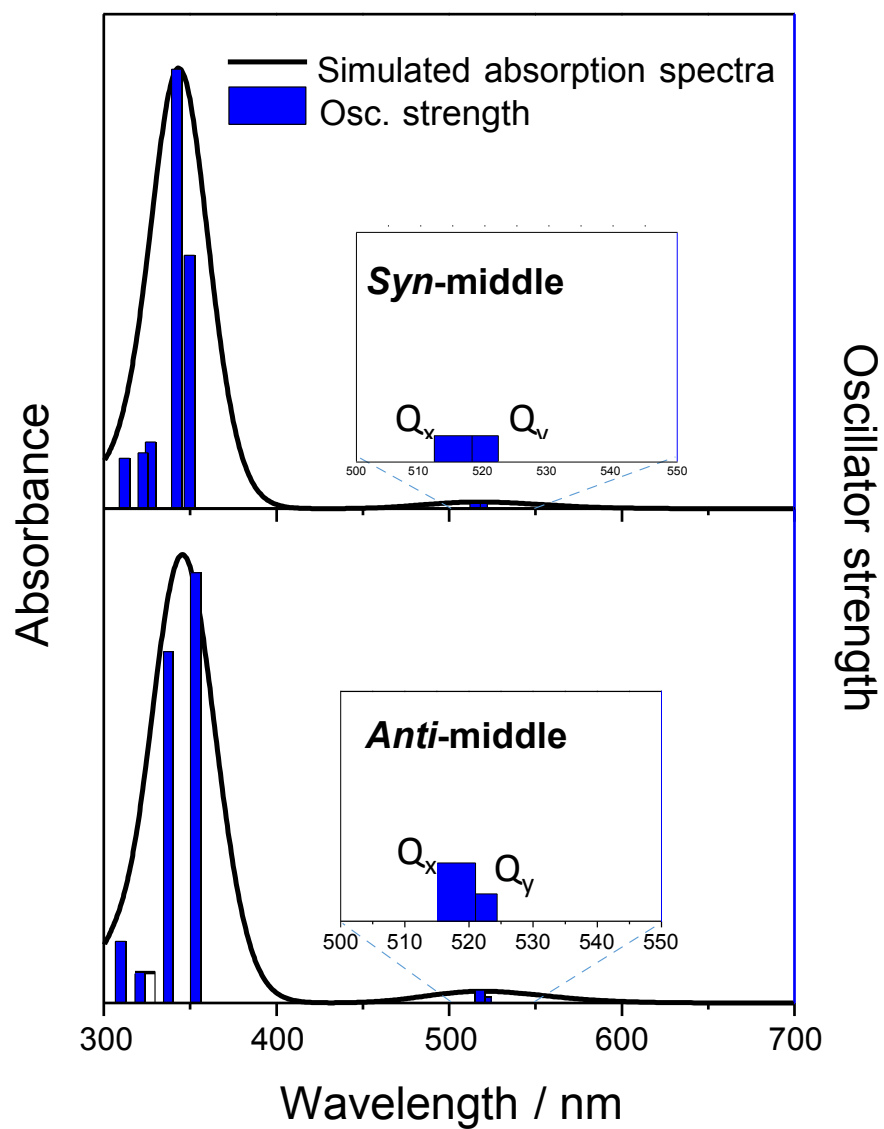


Fig. S6 TDDFT calculation on model compounds (*syn*- and *anti*-middle) are represented.

TDDFT calculation on model compounds

Steady-state fluorescence excitation anisotropy measurements

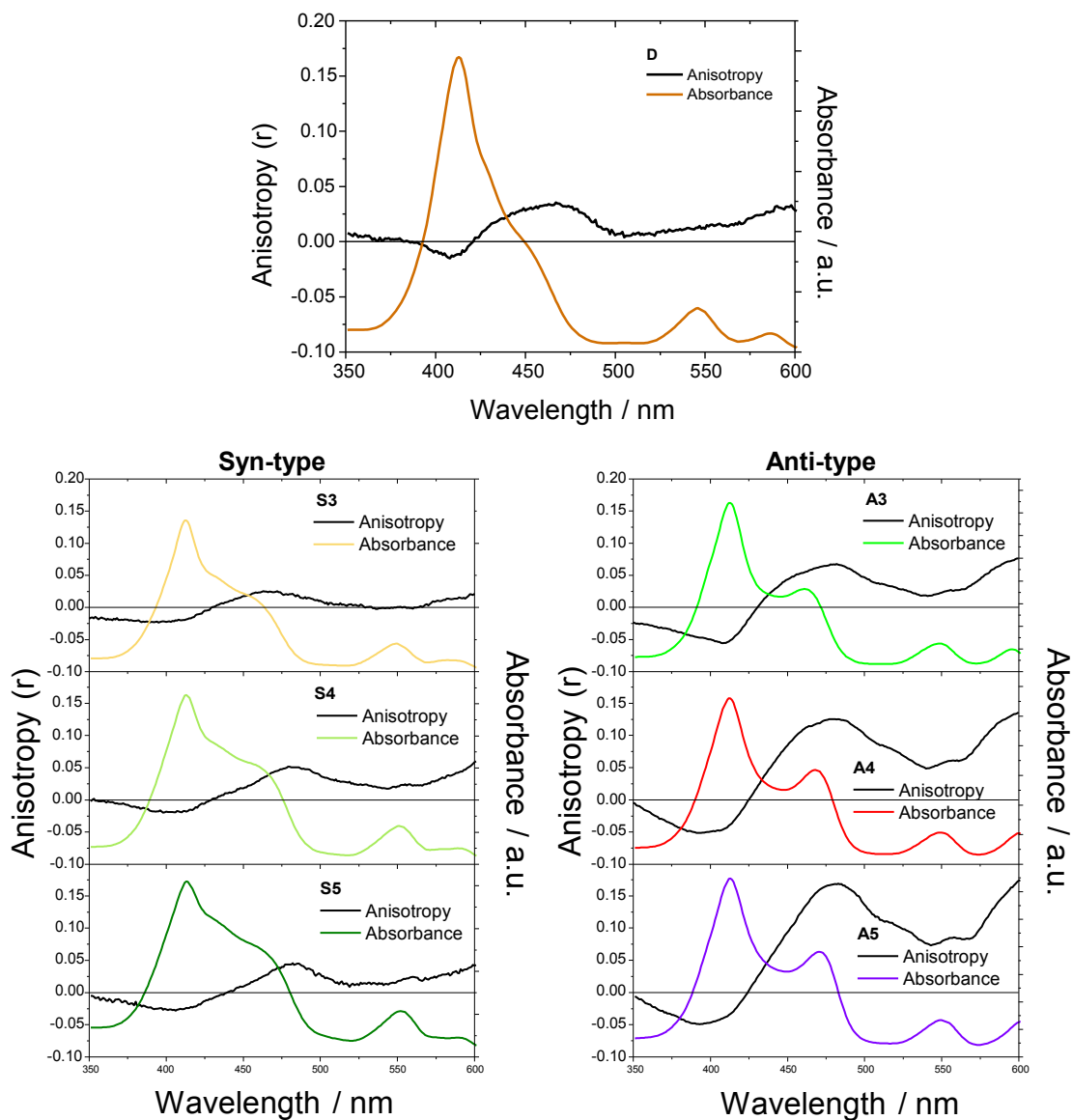


Fig. S7 Steady-state excitation anisotropy measurements for **D** (top), **S_n** (bottom left), and **An** (bottom right) are conducted. Anisotropy values are plotted with their absorption spectra ($\lambda_{em} = 615$ nm).

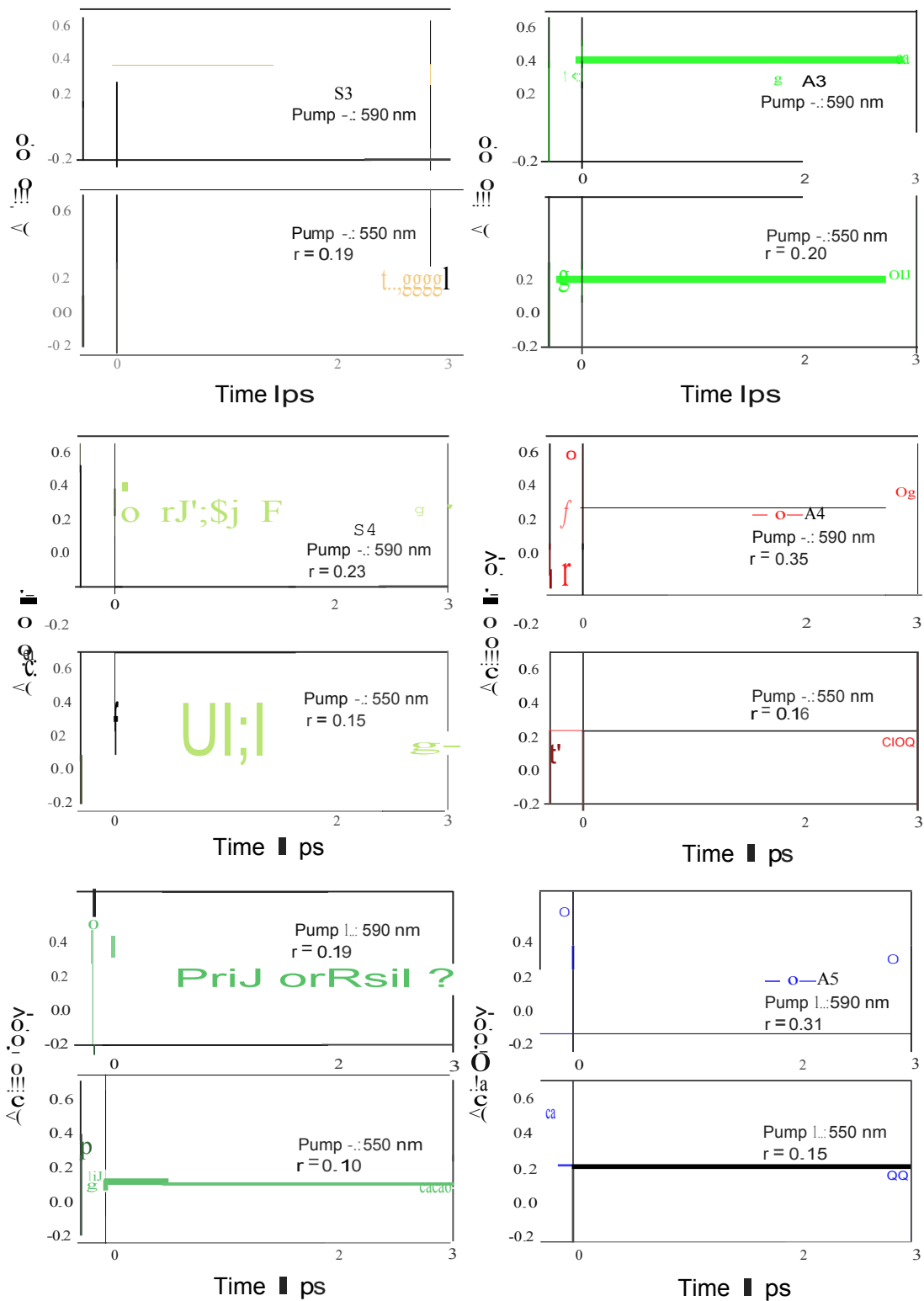


Fig. S8 Transient absorption anisotropy of Sn (left) and An (right) are represented upon two pump wavelength of 550 and 590 nm probing the lowest electronic excited state region denoting with plateau anisotropy values.

Transient absorption anisotropy measurements

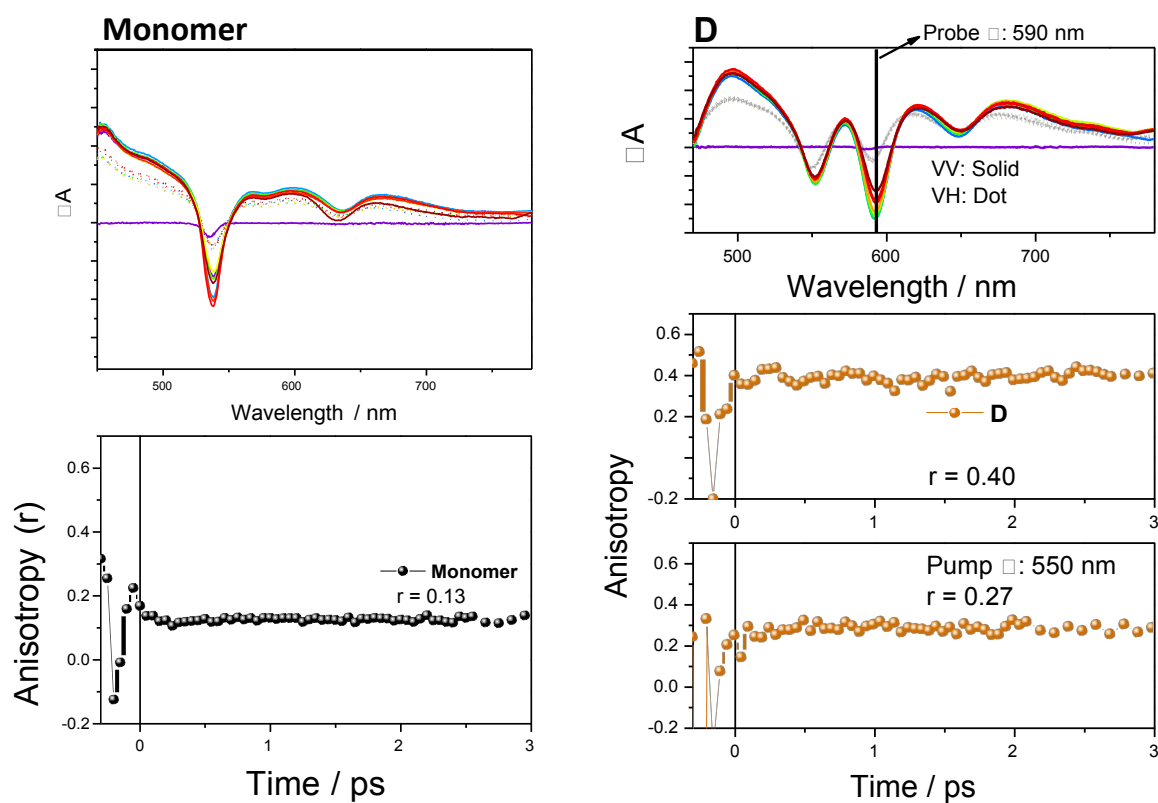


Fig. S9 Transient absorption anisotropy of **M** (left) and **D** (right) are represented. Anisotropy value of **M** is shown (probing 600 nm) which is almost identical with probing range of 480-700 nm. Anisotropy value of **D** is shown by probing the lowest electronic excited state region denoting with plateau anisotropy values.

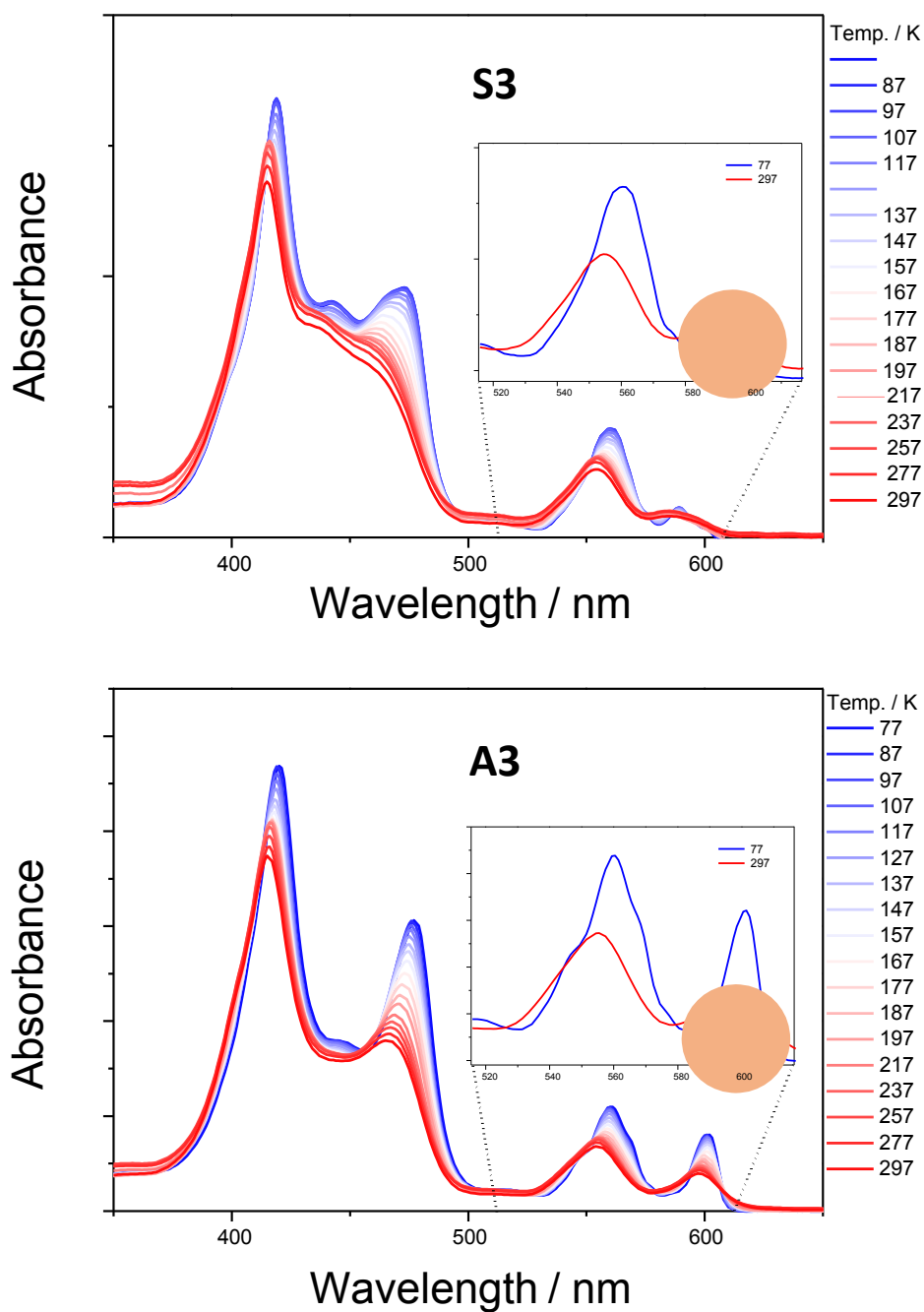


Fig. S10 Temperature controlled absorption spectra of **S3** (top) and **A3** (bottom) were recorded, inset showing absorption spectra at 77 and 297 K in the lowest electronic excited state.

Temperature controlled absorption spectra

Reference

- (1) Jiang, H.-W.; Kim, T.; Tanaka, T.; Kim, D.; Osuka, A. *Chem. Eur. J.* **2016**, *22*, 83–87.
- (2) Frisch, M. J.; Trucks, G. W.; Schlegel, H. B.; Scuseria, G. E.; Robb, M. A.; Cheeseman, J. R.; Scalmani, G.; Barone, V.; Mennucci, B.; Petersson, G. A.; Nakatsuji, H.; Caricato, M.; Li, X.; Hratchian, H. P.; Izmaylov, A. F.; Bloino, J.; Zheng, G.; Sonnenberg, J. L.; Hada, M.; Ehara, M.; Toyota, K.; Fukuda, R.; Hasegawa, J.; Ishida, M.; Nakajima, T.; Honda, Y.; Kitao, O.; Nakai, H.; Vreven, T.; Montgomery, Jr., J. A.; Peralta, J. E.; Ogliaro, F.; Bearpark, M.; Heyd, J. J.; Brothers, E.; Kudin, K. N.; Staroverov, V. N.; Kobayashi, R.; Normand, J.; Raghavachari, K.; Rendell, A.; Burant, J. C.; Iyengar, S. S.; Tomasi, J.; Cossi, M.; Rega, N.; Millam, J. M.; Klene, M.; Knox, J. E.; Cross, J. B.; Bakken, V.; Adamo, C.; Jaramillo, J.; Gomperts, R.; Stratmann, R. E.; Yazyev, O.; Austin, A. J.; Cammi, R.; Pomelli, C.; Ochterski, J. W.; Martin, R. L.; Morokuma, K.; Zakrzewski, V. G.; Voth, G. A.; Salvador, P.; Dannenberg, J. J.; Dapprich, S.; Daniels, A. D.; Farkas, Ö.; Foresman, J. B.; Ortiz, J. V.; Cioslowski, J.; Fox, D. J. *Gaussian 09*, revision A.1; Gaussian Inc.; Wallingford CT, **2009**.
- (3) Yanai, T.; Tew, D. P.; Handy, N. C. *Chem. Phys. Lett.* **2004**, *393*, 51-57.
- (4) Ditchfield, R.; Hehre, W. J.; Pople, J. A. *J. Chem. Phys.* **1971**, *54*, 724-728.